

# Multi-Layer Fringe-Field Augmentations for the Efficient Modeling of Package Power Planes

Krishna Bharath<sup>†</sup>, Nithya Sankaran<sup>¶</sup>, A. Ege Engin<sup>‡</sup> and Madhavan Swaminathan<sup>§</sup>  
 School of Electrical and Computer Engineering  
 Georgia Institute of Technology  
 Atlanta, GA 30332  
 Email: {<sup>†</sup>kbharath, <sup>¶</sup>nithya, <sup>‡</sup>engin, <sup>§</sup>madhavan}@ece.gatech.edu

## Abstract

Modern mixed signal system-on-package integration schemes employ power distribution networks with highly irregular geometries. To model this problem, most techniques resort to approximations which lead to the fringe fields being ignored. In this paper, an efficient modeling method is proposed for multi-layered package power/ground planes with apertures. The solution technique employs the multi-layer finite difference method (M-FDM), with fringe field corrections provided by a 2D electrostatic solver. This scheme allows for efficient frequency domain simulation, and the S-parameters obtained from the method have been compared with full-wave simulations and measurements.

## I. INTRODUCTION

Mixed signal system-on-package (SoP) technology is a key enabler of increasing functional integration, especially in mobile and wireless systems. SoP allows the integration of high speed digital, RF and passive components at a package level, thereby preserving performance at a lower cost compared to system-on-chip based solutions. Due to the presence of multiple dissimilar modules, each having unique power supply requirements, the design of the power distribution network (PDN) becomes critical.

Typically, this PDN is designed as alternating layers of power and ground planes with signal interconnects routed in between or on top of the planes. This arrangement serves two purposes - firstly, it allows a reduction in the package inductance, and secondly, signal lines on separate layers are isolated from each other due to the shielding effect of the planes.

In the case of a SoP module, to provide DC isolation between power supplies, the power and ground planes may be segmented into islands. In this case, EM coupling becomes a critical factor. Consider the SoP containing four modules shown in Figure 1. The digital module is the source of the simultaneous switching noise (SSN) containing harmonics at multiples of the clock frequency. For the case of a cell phone receiver, relatively low insertion loss levels between the digital and RF modules can significantly degrade the performance of the front-end low-noise amplifier. Clearly, time-efficient and accurate signal and power integrity (SI/PI) simulation will be a critical component of the SoP design flow.

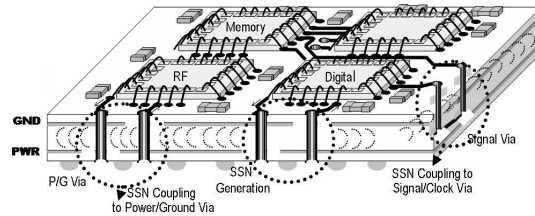


Fig. 1. A system on package module.

An efficient approximation that can be employed for package power planes is that of a planar circuit [1]. A planar circuit is a microwave structure in which one of the three dimensions, say  $z$ , is much smaller than the wavelength. Under this condition, it can be assumed that the field is invariant along the  $z$ -direction. Hence,  $\frac{\delta}{\delta z} = 0$  and the Helmholtz wave equation can be reduced to 2 dimensions as:

$$(\nabla_t^2 + k^2) u = j\omega\mu d J_z, \quad \nabla_t^2 = \left( \frac{\delta^2}{\delta x^2} + \frac{\delta^2}{\delta y^2} \right) \quad (1)$$

where  $\nabla_t^2$  is the transverse Laplace operator parallel to the planar structures,  $u$  is the voltage,  $d$  is the distance between the planes,  $k$  is the wave number, and  $J_z$  is the current density injected normally to the planes [2]. The open circuit at the boundary can be represented by a magnetic wall or Neumann boundary condition, which completes the problem formulation. Two solutions that have been proposed are the multi-layer finite difference method (M-FDM) and the Green's function based segmentation technique.

For either technique, the modeling of PDN geometries is valid for large plane-pairs, where the lateral dimensions are much larger than the dielectric thickness separating the planes. However, in many PDNs, the presence of narrow lines implies that simulation results will be inaccurate. Also, even in the case when metal planes are wide compared to the substrate height, there can be significant coupling that can be associated with the fringe fields from plane edges.

This problem has been considered in [3] for microstrip geometries. Recently, in [4], an extended segmentation approach was proposed, wherein the segmentation approach is coupled with a 2D field solver, such that the effect of discontinuities such as vias can be extracted out. In this paper, the M-FDM method is modified with a fringe augmentation (FA) technique, where the fringe elements are obtained from a 2D electrostatic solution. This technique enables the method to accurately characterize irregular multi-layered packages.

The rest of the paper is organized as follows. In Section II, the multi-layer finite difference method (M-FDM) is briefly explained. The modeling of fringe fields is illustrated in Section III. Model to hardware correlation is shown in Section IV, with conclusions in Section V.

## II. FREQUENCY DOMAIN SOLUTION OF AN IRREGULAR MULTI-LAYER PACKAGE

By applying the finite-difference scheme, the 2-dimensional Laplace operator can be approximated as

$$\nabla_t^2 u_{i,j} = \frac{u_{i,j+1} + u_{i+1,j} + u_{i,j-1} + u_{i-1,j} - 4u_{i,j}}{h^2} \quad (2)$$

, where  $h$  is the mesh length and  $u_{i,j}$  is the voltage at node  $(i,j)$  for the cell-centered discretization shown in Figure 2.

Applying this finite difference scheme leads to a system of KCL equations that result in the well known bedspring model. The extension of this formulation to multi-layer geometries is described in [5].

Following the formulation provided in [5], the total unit cell can be obtained as shown in Figure 3(b) for the example of three planes, where the bottom plane is chosen as the voltage reference plane. The equivalent circuit that would be obtained for a three layer geometry is shown in Figure 3(c). For solid multilayered rectangular planes, discretized with  $M_1$  cells in the  $x$ -direction and with  $M_2$  cells in the  $y$ -direction, the admittance matrix  $\overline{\overline{Y}}$  can be written as

$$\overline{\overline{Y}} = \begin{pmatrix} \overline{\overline{A}} & \overline{\overline{B}} & & & \\ \overline{\overline{B}} & \overline{\overline{A}} - \overline{\overline{B}} & \overline{\overline{B}} & & \\ & \overline{\overline{B}} & \ddots & \ddots & \\ & & \ddots & \ddots & \overline{\overline{B}} \\ & & & \overline{\overline{B}} & \overline{\overline{A}} \end{pmatrix} \quad (3)$$

Here,  $A$  and  $B$  are  $kM_1 \times kM_1$  matrices for  $(k+1)$  planes, assuming that the nodes are numbered starting from the top node in the lowest row, increasing in the vertical direction to the bottom node, then starting with the next cell in the  $x$ -direction until the last cell, and then starting with the next row. Hence,  $\overline{\overline{Y}}$  is a  $(kM_1M_2) \times (kM_1M_2)$  matrix.

The matrix solution technique can be enhanced by the use of nested dissection, which is an asymptotically optimal node ordering method [6]. It can be shown that the computational complexity of M-FDM applied to  $k+1$  layers is  $O(N^{1.5})$  and with a memory requirement of  $O(N \log_2 N)$  [7].

## III. ADDITION OF FRINGE ELEMENTS TO M-FDM

At distances far away from the plane edges (approximately  $> 10h$ ), the E-field is predominantly oriented along the  $z$ -axis. However, significant fringing can occur close to the edges. These fields can be modeled by the fringe augmentation (FA) method coupled with the M-FDM formulation as follows:

Firstly, a cross-section of the package perpendicular to the edge is obtained. Secondly, this cross-section is analyzed with a 2D electrostatic solver to obtain the per-unit-length (p.u.l) capacitance and inductance matrices.

A finite-element scheme using a triangular mesh with  $N$  nodes and rooftop basis functions is applied to Laplace's equation,  $\nabla \cdot (\epsilon \nabla u) = 0$ , where  $u$  is the potential distribution in the cross-section. We obtain and solve the system:

$$\sum_{j=1}^N \left( \int_{\Omega} (\epsilon \nabla \Phi_j) \cdot \nabla \Phi_i \right) U_j = 0, \quad i, j = 1, 2, \dots, N \quad (4)$$

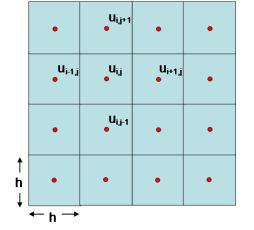


Fig. 2. Discretization of the Laplace operator.

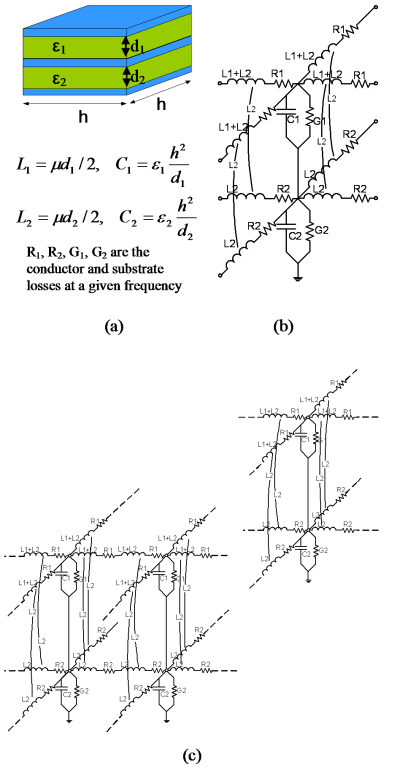


Fig. 3. (a) Geometry and p.u.c. parameters. (b) Combined unit cell model for three planes. (c) Plane model consisting of multilayer unit cells.

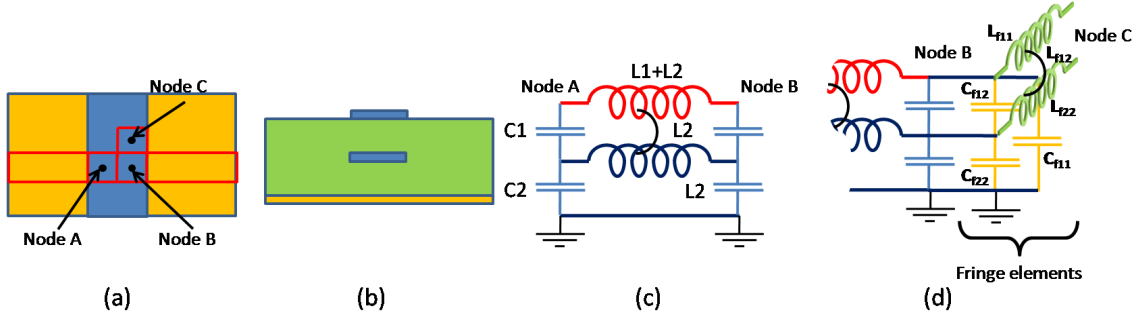


Fig. 4. Addition of Fringe elements. (a) Top view of top and middle layers (b) Cross section (c) M-FDM circuit model between Nodes A and B (d) Circuit model as a result of fringe augmentation (FA).

where  $\Phi_i$  is the rooftop basis and  $U_i$  is the unknown potential, defined at node  $i$ . The capacitance matrix,  $\overline{\overline{C}}_{2D}$ , can be obtained by applying Gauss' law:

$$C_{i,j} = \oint_{l_j} \epsilon \frac{\delta V}{\delta n} dl_j \quad (5)$$

, where  $C_{i,j}$  is the  $(i,j)^{th}$  entry in the capacitance matrix, found by integrating the normal component of the potential gradient around a contour  $l_j$  enclosing the  $j^{th}$  conductor with a 1V potential applied to the  $i^{th}$  conductor. The high frequency inductance matrix,  $\overline{\overline{L}}_{2D}$ , can be found to be  $\sqrt{\mu_0 \epsilon_0} \overline{\overline{C}}_{2D0}^{-1}$ , where  $\overline{\overline{C}}_{2D0}^{-1}$  is the capacitance matrix of the same structure in vacuum.

While  $\overline{\overline{C}}_{2D}$  and  $\overline{\overline{L}}_{2D}$  represent the correct p.u.l capacitance and inductance of the structure, due to the approximation  $\frac{\delta}{\delta z} = 0$  used by the formulation, as described earlier, the p.u.l inductance and capacitance of the M-FDM model represent only the contributions from the parallel plate fields. We denote these capacitance matrices as  $\overline{\overline{C}}_{pp}$  and  $\overline{\overline{L}}_{pp}$ .

Once  $\overline{\overline{C}}_{2D}$  and inductance  $\overline{\overline{L}}_{2D}$  are obtained, they can be used to derive the fringe augmentation (FA) elements  $\overline{\overline{C}}_f$  and  $\overline{\overline{L}}_f$ .  $\overline{\overline{C}}_f$  represents the additional capacitive elements to be added to  $\overline{\overline{Y}}$  to correctly model the fringe E-fields.  $\overline{\overline{L}}_f$  represents additional inductive elements to be added between adjacent nodes that lie parallel to the edge being considered, to correctly model the fringe H-fields.

Given that  $\overline{\overline{C}}_f$  and  $\overline{\overline{L}}_f$  are added symmetrically on the two sides of the cross-section being considered, we obtain the following relations:

$$\overline{\overline{C}}_{2D} = \overline{\overline{C}}_{pp} + 2 \frac{\overline{\overline{C}}_f}{w}, \text{ where } w \text{ is the discretization width} \quad (6)$$

and

$$\overline{\overline{L}}_{2D}^{-1} = \overline{\overline{L}}_{pp}^{-1} + 2w \overline{\overline{L}}_f^{-1} \quad (7)$$

From the above equations, we obtain the expressions for  $\overline{\overline{C}}_f$  and  $\overline{\overline{L}}_f$ :

$$\overline{\overline{C}}_f = \frac{1}{2} (\overline{\overline{C}}_{2D} - \overline{\overline{C}}_{pp}) w \quad (8)$$

and

$$\overline{\overline{L}}_f = 2 \left( \overline{\overline{L}}_{2D}^{-1} - \overline{\overline{L}}_{pp}^{-1} \right)^{-1} w \quad (9)$$

As an illustration, consider a three metal layer geometry, the top view of which is shown in Figure 4(a). To provide a simple explanation of the FA method, only three nodes (A, B and C) in the finite difference mesh are considered. To include the matrix entries associated with the fringe field, the cross section of the structure, as shown in Figure 4(b) is considered. The bottom conductor is considered to be the reference conductor, and hence,  $\overline{\overline{C}}_f$  and  $\overline{\overline{L}}_f$  will be  $2 \times 2$ . In Figure 4(c), the circuit elements between Nodes A and B are shown, as derived from the M-FDM formulation. The correction of the system matrix,  $\overline{\overline{Y}}$ , with the elements from the FA matrix  $\overline{\overline{C}}_f$  and  $\overline{\overline{L}}_f$  results in the addition of new circuit elements as shown in Figure 4(d).

It can be noted that since no new non-zeros are being added to  $\overline{\overline{Y}}$ , the matrix factorization and solve time remain unchanged.

#### IV. RESULTS

The M-FDM technique with fringe augmentations was used to analyze two test structures. All simulations were carried out on an Intel dual-Xeon workstation with 3 GB of RAM. An Agilent four port, 40 GHz VNA was used for measurements. The full-wave method-of-moments based tool, EMSurf, which is a part of the IBM EIP suite has also been used for correlation [8].

The first test structure contains three metal layers with 30 mm wide planes in the top and middle layers. The top view of this structure is shown in Figure 5(a), with the cross section in Figure 5(b). The dielectric was FR-4 with 200  $\mu\text{m}$  thickness and  $\tan \delta$  of 0.015. Port locations are indicated by the circles shown in Figure 5(a). Also, as can be seen by the arrows in Figure 5(b), the terminals of Port 1 are connected between the top and middle layers, while the terminals of Port 2 are connected between the middle and bottom layers.

The insertion loss results are provided in Figure 5(c). When the fringe augmentations are not included, M-FDM [5] simulations indicate that the ports are uncoupled. Hence, the insertion loss between the ports is negligible. When the fringe augmentations are included, there is good agreement with the full-wave EM solution. Also, a significantly high  $S_{21}$  of -8dB at 2.4 GHz has been captured.

The second test case also contains three metal layers with identically shaped apertures on the top and middle layers. The top view for these layers is shown in Figure 6(a) and the cross section is shown in Figure 6(b). The dielectric layers are 50  $\mu\text{m}$  thick with a relative permittivity of 3.4 and  $\tan \delta$  of 0.06, with 20  $\mu\text{m}$  thick metal layers. Port locations are indicated by the circles shown in Figure 6(a), and as in the previous case, the terminals of Port 1 are connected between the top and middle layers, while the terminals of Port 2 are connected between the middle and bottom layers.

As before, when the fringe augmentations are not included, M-FDM simulations indicate that the ports are uncoupled. As seen from the insertion loss results shown in Figure 6(c), there is a good agreement between the M-FDM technique with fringe augmentations, the full-wave EM solution and measurement.

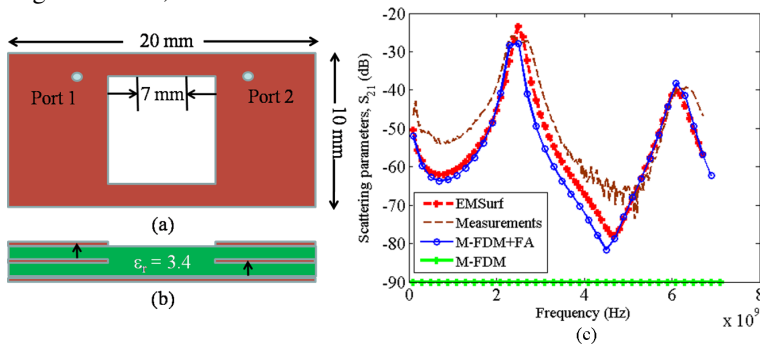


Fig. 6. Geometry of multilayer test structure II. (a) Top view of top and middle layers (b) Cross section (c) Insertion Loss.

an efficient hybrid method to model these fringe fields has been proposed. The technique uses the multi-layer finite difference method (M-FDM) to provide an initial model for the package. Next, a 2D electrostatic solver is used to extract and correct only the matrix entries for nodes that lie on metal edges. This technique has been compared for accuracy against a full-wave EM simulator and measurements, and has shown to be critical. The efficiency of the technique can be further improved by localizing the electrostatic solution to the metal edges, since the extracted values of the fringe and gap components are relatively constant for wide planes. Thus, even a complex geometry requires relatively few 2D solutions.

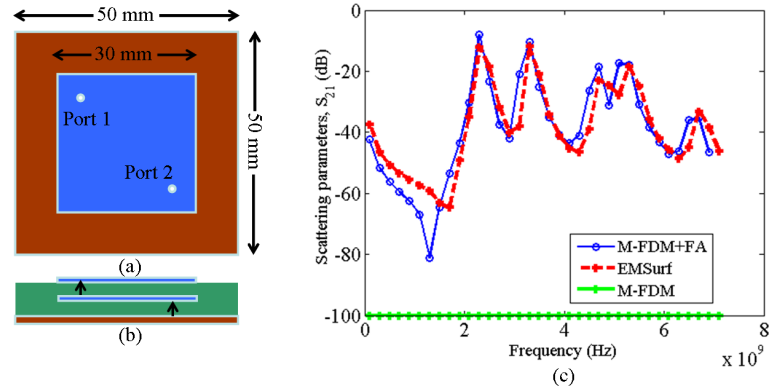


Fig. 5. Geometry of multilayer test structure I. (a) Top view of top and middle layers (b) Cross section (c) Insertion Loss.

For this case, there are two non-unique cross sections to be considered for 2D analysis to obtain the fringe inductance and capacitance matrices. These simulations required about 10s each. The M-FDM simulations contained 14,400 cells and required 0.44s per frequency point.

## V. CONCLUSIONS

In modern mixed-signal systems integrated using a multi-layered SoP-based technology, the accurate modeling of the PDN is critical. Most efficient full-package modeling methods ignore the effect of fringe fields which can lead to loss in accuracy. In this paper,

## REFERENCES

- [1] T. Okoshi and T. Miyoshi, "The planar circuit - an approach to microwave integrated circuitry," *IEEE Trans. Microwave Theory Tech.*, vol. MTT-20, pp. 245–252, April 1972.
- [2] E. T. Itoh, *Numerical Techniques for Microwave and Millimeter-Wave Passive Structures*. John Wiley, 1989.
- [3] K. Bharath, E. Engin, M. Swaminathan, K. Uriu, and T. Yamada, "Efficient modeling of package power delivery networks with fringing fields and gap coupling in mixed signal systems," in *Proc. of 15th IEEE EPEP*, Oct. 2006, pp. 59–62.
- [4] V. Kollia and A. C. Cangellaris, "Extended segmentation procedure for electromagnetic modeling of the power distribution network," in *Proc. of IEEE EPEP 2007*, Oct. 2007, pp. 65 – 68.
- [5] A. Engin, K. Bharath, M. Swaminathan, and et. al., "Finite-difference modeling of noise coupling between power/ground planes in multilayered packages and boards," in *Proc. of 56th ECTC*, June 2006, pp. 1262 – 1267.
- [6] A. George, "Nested dissection of a regular finite element mesh," *SIAM Journal on Numerical Analysis*, vol. 10, no. 2, pp. 345–363, April 1973.
- [7] K. Bharath, E. Engin, M. Swaminathan, K. Uriu, and T. Yamada, "Computationally efficient power integrity simulation for system-on-package applications," in *Proc. of 44th DAC*, July 2007, pp. 612 – 617.
- [8] <http://www.alphaworks.ibm.com/tech/eip>